Title

Representation of Vapor-Liquid and Liquid-Liquid Equilibria for Binary Systems Containing Polymers: Applicability of an Extended Flory-Huggins Equation

Authors

Bae, Y.C.
Shim, J.J.
Soane, D.S.
et al.

Publication Date

1991-09-01

LBL-31891
UC-401
Preprint

Lawrence Berkeley Laboratory
UNIVERSITY OF CALIFORNIA

CHEMICAL SCIENCES DIVISION

Submitted to Journal of Applied Polymer Science

Representation of Vapor-Liquid and Liquid-Liquid Equilibria for Binary Systems Containing Polymers: Applicability of an Extended Flory-Huggins Equation

Y.C. Bae, J.J. Shim, D.S. Soane, and J.M. Prausnitz

September 1991

Prepared for the U.S. Department of Energy under Contract Number DE-AC03-76SF00098

LBL-31891

UC-401

Representation of Vapor-Liquid and Liquid-Liquid Equilibria for Binary Systems Containing Polymers. Applicability of an Extended Flory-Huggins Equation

Y. C. Bae, J. J. Shim, D. S. Soane and J. M. Prausnitz

Department of Chemical Engineering
University of California

and

Chemical Sciences Division
Lawrence Berkeley Laboratory
1 Cyclotron Road
Berkeley, CA 94720

This work was supported by the Director, Office of Energy Research, Office of Basic Energy Sciences, Chemical Sciences Division of the U.S. Department of Energy under Contract Number DE-AC03-76SF00098. Additional funding was provided by E. I. du Pont de Nemours & Co., Enichem Polimeri, Koninklijke Shell, and ATOCHEM.

Representation of Vapor-Liquid and Liquid-Liquid Equilibria for Binary Systems Containing Polymers.

Applicability of an Extended Flory-Huggins Equation.

Y. C. Bae, J. J. Shim, D. S. Soane, and J. M. Prausnitz

Department of Chemical Engineering, University of California and Chemical Sciences Division, Lawrence Berkeley Laboratory Berkeley, California 94720

ABSTRACT: For some binary systems, an extended Flory-Huggins equation is applicable to both vapor-liquid equilibria (VLE) and liquid-liquid equilibria (LLE) using the same adjustable parameters. New LLE and VLE data are reported for polystyrene (PS) (MW = 100,000)/cyclohexane and for poly(ethylene glycol) (PEG) (MW = 8,000)/water. Experimental results for the PS/cyclohexane system agree well with the semi-empirical model, while those for PEG/water do not, probably because, for PEG/water, the temperature range of the VLE data is about 55 °C lower than that of the LLE data. Excellent fits were obtained for our previously published experimental results for PS/cyclohexane (upper critical solution temperature, UCST), PS/ethyl acetate (lower critical solution temperature, LCST), PS/*tert*-butyl acetate and PS/methyl acetate (both UCST and LCST), and PEG/water (closed-loop). The semi-empirical model also fits well new data obtained for the polymer blend PS/poly(vinyl methyl ether).

Introduction

Understanding the phase behavior of polymer solutions and blends is important for the development, production and processing of polymeric materials. In this study, we discuss application of a semi-empirical molecular-thermodynamic framework for correlating phase equilibria in some binary polymer/solvent systems and in one binary polymer/polymer system. The correlation is applicable to both vapor-liquid (VLE) and liquid-liquid equilibria (LLE) at temperatures commonly encountered in industrial processes.

A variety of polymer-solution theories has been developed during the last half century. The best known is the Flory-Huggins lattice theory.[1] In the simplest version of that theory, the interaction parameter (χ_{FH}) is independent of composition and inversely proportional to temperature. However, extensive experimental results by many researchers show clearly that for most polymer-containing systems, χ_{FH} is a function of polymer concentration and that its temperature dependence is not a simple proportionality to inverse temperature.

While much work has been reported for VLE, the literature has given less attention to fundamental studies on LLE for polymer-containing systems. We cannot give a complete literature review here but mention only a few relatively recent publications.

Freed and coworkers[2-6] have developed a lattice-field theory for polymer solutions which, in principle, provides an exact mathematical solution of the Flory-Huggins lattice. In this theory, good agreement was found between calculated values and the computer simulation data by Dickman and Hall[7] for the chain-insertion probability and for pressures in a system of athermal chains and voids.

Hu and coworkers[8] reported a double-lattice model for the Helmholtz energy of mixing for binary polymer solutions based on Freed's lattice-field theory. This model takes specific interactions into account.

To account for compressibility and density changes upon isothermal mixing, Sanchez and Lacombe[9-10], and Koningsveld and Kleintjens[11], have developed different forms of a lattice-fluid model based on Flory-Huggins theory. Sanchez and Balazs[12] introduced corrections for oriented interactions between dissimilar components. Recently, Panayiotou and Sanchez[13] have modified the lattice-fluid theory for polymer solutions to account for strong interactions (hydrogen bonding) between polymer and solvent. Their model is in the form of an equation of state suitable for describing thermodynamic properties of polymer solutions over an extended range of external conditions from the ordinary liquid state up to high temperatures and pressures where the solvent may be supercritical.

Free-volume theories for polymer solutions were developed by numerous investigations, notably by Flory[14] and by Patterson and Delmas[15].

In a recent publication, Qian and coworkers[16-17] have returned to the original Flory-Huggins lattice theory using a χ parameter which is given by the product of two functions, one depending on composition and the other on temperature. This semi-empirical theory permits fitting most observed types of binary liquid-liquid phase diagrams (UCST, LCST, UCST and LCST, hourglass, and closed loop) by adjusting the temperature- and concentration-dependent coefficients. Qian et al, however, did not consider VLE.

In this study, we slightly simplified Qian's model. With some success, we apply our version of that model to both VLE and LLE using the same adjustable parameters for a given binary system.

Experimental

Vapor-liquid equilibria. VLE for several binary polymer solutions were measured using a Cahn D-200 Digital Recording Balance Sorption Apparatus (Figure 1) which is sensitive to changes as small as 0.1 microgram. This apparatus consists of three major sections: the weighing system (balance), the vapor-delivery system and the data-acquisition system (computer). The weighing unit of the balance produces an electric current which corresponds to the weight of the sample. These signals are transferred to the weighing unit and are amplified, digitized, filtered for noise, temperature compensated, calibrated and then converted into a format which can be read by a computer. The computer (IBM 286 Personal Computer) shows the weight change on the screen and stores it in the hard disk. The vapor delivery system delivers a solvent vapor to the balance chamber.

Procedure for VLE measurement. An empty sample bowl is placed in the balance chamber. It is dried completely by evacuating at a constant temperature until the weight remains constant (valves 5 and 9 are closed and the others are open). The weight of the empty bowl is measured at different pressures of pure nitrogen (valves 1,2,3,10 and 11 are open and the others are closed). Pure nitrogen was supplied into the balance chamber by opening valve 12. The balance chamber is evacuated and the solvent vapor is supplied to the chamber to correct for adsorption of solvent on the sample pan and for buoyancy (valves 3,4,9 and 12 are closed and the others are open). The sorption of solvent in the polymer was measured in the same way as that for the empty sample bowl at the same condition with a polymer sample of about 10 mg on the bowl. Every weighing was done after isolating the balance chamber (valves 1 and 2 are closed) from the pump and the solvent flask. The amount of absorption of the solvent into the polymer is calculated from the amount of sorption by subtracting the amount of adsorption on the sample bowl and the buoyancy effect at the same pressure and temperature.

The temperature of the water bath for the water jacket remains constant throughout the series of runs. The temperature of the solvent flask is set about 0.2 °C higher than the boiling point of the solvent at the prevailing pressure and is maintained well within ±0.1 °C in the water bath by agitating with a magnetic stirrer. The pressure of the system is controlled by applying a constant vacuum (0.001 mmHg) and by a mercury pressure controller (Cartesian-Diver-type Absolute Pressure Controller GC-2200D from Gilmont Instruments,Inc.) which controls the absolute pressure from 1 mmHg to 50 psi within ±0.2 % of the reading or ±0.1 mmHg, whichever is greater. Pressure is read from a U-tube mercury manometer with an uncertainty of no more than ±0.2 mmHg. The manometer was calibrated to compensate the density change of mercury with temperature using an accurate barometer. The overall experimental error in weight change of polymer was less than ±3%.

We have measured VLE for polystyrene (MW = 100,000) /cyclohexane at 30, 40, 50, and 60 °C and for poly(ethylene glycol)/water for 50, 60, and 70 °C. Here PS stands for polystyrene and PEG stands for poly(ethylene glycol).

Liquid-liquid equilibria. The cloud-point curves of binary polymer solutions were determined by a thermo-optical analysis method at the saturated vapor pressure as described in ref. 19. We measured these systems: PS in cyclohexane, methyl acetate, *tert*-butyl acetate, and ethyl acetate and PEG in water.

Polymer blends. PS samples were used as received from Polysciences, Inc. and poly(vinyl methyl ether) (PVME) was obtained from Scientific Polymer Products, Inc. A series of blends of PS/PVME was prepared by dissolving the known composition of the dried blend powders in toluene. This solution (5 w.t. % total polymer) was cast onto a microscope slide in the oven at room temperature. These cast films were further dried under vacuum at 90 °C for at least 48 hrs. Cloud-points were determined by a thermo-optical analysis method as discussed earlier.[19]

Correlating Equations

For a binary polymer solution, the Flory-Huggins expression for ΔG, the molar Gibbs energy of mixing at temperature T, is given by[1]

$$\frac{\Delta G}{RT} = \frac{\phi_1}{r_1}\ln\phi_1 + \frac{\phi_2}{r_2}\ln\phi_2 + \chi_{FH}\phi_1\phi_2 \qquad (1)$$

where R is the gas constant, ϕ_1, ϕ_2, r_1, and r_2 are the volume fractions and relative molar volumes of component 1 and 2, respectively, and χ_{FH} is the Flory-Huggins interaction parameter; r_2 is defined by

$$r_2 = \frac{v_2 MW_2}{v_1 MW_1} \qquad (1)'$$

where v_1, v_2, MW_1, and MW_2 are specific volumes of solvent and polymer and molecular weights of solvent and polymer, respectively; $r_1 = 1$ for solvent.

In the original Flory-Huggins equation, χ_{FH} is only a function of temperature. However, it has been known for many years that χ depends on both temperature and concentration[20-23]. Recently, Qian, Mumby and Eichinger[16,17] suggested a semi-empirical form for χ. They replaced χ_{FH} by $g(T,\phi_2)$, a function of temperature and concentration. Their Gibbs energy function is given by

$$\frac{\Delta G}{RT} = \frac{\phi_1}{r_1}\ln\phi_1 + \frac{\phi_2}{r_2}\ln\phi_2 + g(T,\phi_2)\phi_1\phi_2 \qquad (2)$$

The relationship between g and χ is derived from the chemical potential. Relative to pure component 1, the chemical potential $\Delta\mu_1$ of component 1 in the solution is defined by

$$\Delta\mu_1 = \left(\frac{\partial \Delta G}{\partial n_1}\right)_{T,P,n_2} \quad (3)$$

and a similar relation holds for $\Delta\mu_2$. The chemical potentials of components 1 and 2 can be derived from eqs. 2 and 3; they are

$$\frac{\Delta\mu_1}{RT} = \ln(1-\phi_2) + \phi_2\left(1-\frac{r_1}{r_2}\right) + \phi_2^2 r_1 g - \phi_1\phi_2^2 r_1 g' \quad (4)$$

$$\frac{\Delta\mu_2}{RT} = \ln\phi_2 + (1-\phi_2)\left(1-\frac{r_2}{r_1}\right) + (1-\phi_2)^2 r_2 g + \phi_1^2\phi_2 r_2 g' \quad (5)$$

where $g' = \left(\frac{\partial g}{\partial \phi_2}\right)_T$.

The interaction parameter, χ, is defined by $\Delta\mu_1$ as[24]

$$\chi = \frac{\Delta\mu_1}{r_1\phi_2^2 RT} - \frac{\ln(1-\phi_2) + \phi_2\left(1-\frac{r_1}{r_2}\right)}{r_1\phi_2^2} \quad (6)$$

Comparing eq. 4 with eq. 6, we have[20]

$$\chi = g - \phi_1 g'. \quad (7)$$

Upon integration at constant temperature,

$$\int_{\phi_2}^{1} \chi(T,\phi)\,d\phi = \int_{\phi_2}^{1} (g - \phi_1 g')\,d\phi = (1-\phi_2)g(T,\phi_2) \quad (8)$$

Function g and the original Flory parameter χ_{FH} are equal only if g is independent of concentration.

The Gibbs energy and chemical potentials in terms of the new interaction parameter χ are given by

$$\frac{\Delta G}{RT} = \frac{1-\phi_2}{r_1}\ln(1-\phi_2) + \frac{\phi_2}{r_2}\ln\phi_2 + \phi_2\int_{\phi_2}^{1}\chi(T,\phi)\,d\phi \tag{9}$$

$$\frac{\Delta\mu_1}{RT} = \ln(1-\phi_2) + \phi_2\left(1-\frac{r_1}{r_2}\right) + \chi(T,\phi_2)r_1\phi_2^2 \tag{10}$$

$$\frac{\Delta\mu_2}{RT} = \ln\phi_2 + (1-\phi_2)\left(1-\frac{r_2}{r_1}\right) + r_2\phi_1\phi_2\chi(T,\phi_2) + r_2\int_{\phi_2}^{1}\chi(T,\phi)\,d\phi \tag{11}$$

Qian et al proposed that χ is given by the product of a temperature dependent term, D(T), and a concentration-dependent term, $B(\phi)$[25]:

$$\chi(T,\phi) = D(T)B(\phi_2) \tag{12}$$

Following Flory[1], Qian et. al.[16,17] suggest

$$D(T) = d_0 + d_1/T + d_2\ln T \tag{13}$$

where d_0, d_1, and d_2 are constants for a given binary system. For the concentration-dependent term, they use

$$B(\phi_2) = 1 + b_1\phi_2 + b_2\phi_2^2 \tag{14}$$

where b_1 and b_2 are constants for a given binary system.

In this study, we use a simple function of concentration:

$$B(\phi_2) = \frac{1}{1-b\phi_2} \tag{15}$$

where b is a binary constant. Eq. 15, with only one adjustable parameter, is sufficient for our purposes.

Binodal. The conditions for equilibrium between two phases in a binary system are given by

$$\mu_1^{\alpha} = \mu_1^{\beta} \tag{16}$$

$$\mu_2^{\alpha} = \mu_2^{\beta} \tag{17}$$

where α and β denote two phases at equilibrium.

The binodal is obtained by combining eqs. 10, 11, 12, 16, and 17, yielding

$$\ln\left(\frac{1-\phi_2^{\beta}}{1-\phi_2^{\alpha}}\right) + (\phi_2^{\beta} - \phi_2^{\alpha})\left(1 - \frac{r_1}{r_2}\right) + r_1 D(T)\left[B(\phi_2^{\beta})(\phi_2^{\beta})^2 - B(\phi_2^{\alpha})(\phi_2^{\alpha})^2\right] = 0 \tag{18}$$

$$\ln\left(\frac{\phi_2^{\beta}}{\phi_2^{\alpha}}\right) + (\phi_2^{\alpha} - \phi_2^{\beta})\left(1 - \frac{r_2}{r_1}\right) + r_2 D(T)\left[B(\phi_2^{\beta})\phi_2^{\beta}\phi_1^{\beta} - B(\phi_2^{\alpha})\phi_1^{\alpha}\phi_2^{\alpha} - \int_{\phi_2^{\beta}}^{\phi_2^{\alpha}} B(\phi)\, d\phi\right] = 0 . \tag{19}$$

The binodal curve is obtained upon simultaneous solution of Equations 18 and 19.

Critical point. The critical condition is given by

$$\frac{\partial \Delta\mu_1}{\partial \phi_2} = \frac{\partial^2 \Delta\mu_1}{\partial \phi_2^2} = 0 \tag{22}$$

The critical temperature and critical volume fraction can be obtained by solving the following two equations simultaneously:

$$\frac{1}{1-\phi_2} - \left(1 - \frac{r_1}{r_2}\right) - r_1\phi_2[\phi_2 B'(\phi_2) + 2B(\phi_2)]D(T) = 0 \tag{23}$$

$$-\frac{1}{(1-\phi_2)^2}+r_1\left[2B(\phi_2)+4\phi_2B'(\phi_2)+\phi_2^2B''(\phi_2)\right]D(T)=0 \tag{24}$$

where $B''(\phi_2)$ is the second derivative of $B(\phi_2)$, with respect to ϕ_2.

Activity of solvent. From the chemical potential, we obtain the activity of the solvent, a_1:

$$\ln a_1=\frac{\Delta\mu_1}{RT}=\ln(1-\phi_2)+\phi_2\left(1-\frac{r_1}{r_2}\right)+\chi(T,\phi_2)r_1\phi_2^2 \tag{25}$$

Since the pure solvent has been chosen as the standard state, $a_1 = P/P_1°$, to the approximation that the vapor is an ideal gas. P is the system pressure and $P_1°$ is the vapor pressure of the pure solvent at system temperature.

Results and Discussion

Tables I gives new experimental cloud-point data for the system PS/poly(vinyl methyl ether). Table II gives new LCST data for the system PS(MW = 100,000)/cyclohexane. Tables III and IV give new experimental VLE data for PS/cyclohexane and for PEG/water, respectively.

Tables V-X give adjustable parameters for each system studied here. Cloud-point curves for binary polymer solutions are reported elsewhere.[19] Constant d_2 in eq. 13 is equal to zero for those systems where only a LCST or a UCST is observed. We used all four adjustable parameters (b, d_0, d_1, d_2) to represent binary systems exhibiting both UCST and LCST or closed-loop phase behavior.

As yet, there are no reliable molecular-thermodynamic models that apply to both VLE and LLE using the same adjustable parameters for a given binary system. In this study, for a few binary systems, we examine the ability of our model to represent both VLE and LLE using the same adjustable parameters for a given binary system.

We have measured both VLE and LLE for PS/cyclohexane (MW = 100,000 for PS) and PEG/water (MW = 8,000 for PEG). Figures 2 and 3 show cloud-point data for PS/cyclohexane systems. In Figure 2, only UCST data are shown; solid lines are calculated from eqs. 18 and 19. The calculated curves provide good fits to the experimental data for all PS samples.

We measured both LCST and UCST data only for PS 100,000 molecular weight. Table II shows experimental cloud-point data for LCST of molecular weight of PS 100 x 10^3. Figure 3 shows the comparison of calculated curves and experimental data for both UCST and LCST. Calculated curves fit the experimental data well.

Figure 4 shows VLE data for the same system at different temperatures. First, we calculated VLE using adjustable parameters obtained from UCST data only. As shown in Figure 4, there is a slight deviation between our predictions and experiment, probably because we did not use also LCST data to obtain the adjustable parameters. Second, we calculated VLE using adjustable parameters obtained from both UCST and LCST data. We expect that LCST curves exist also for other molecular weight of PS. Figure 5 shows a big improvement when compared with Figure 4. Calculated χ agrees better with experiment at the higher temperature, as expected, because if we consider the UCST (21.0 °C) for the system, χ's at 30 °C are closer to the phase boundary of the system which is near the unstable region.

If we consider only UCST data, all adjustable parameters depend on the chain length of the polymer, as shown in Table V. Constant d_0 increases, while constant d_1 decreases with molecular weight of polymer. Constant b depends on the critical composition of the system.

Cloud-point curves for the PEG/water systems are shown in Figure 6. Molecular weights of PEG are 3.35, 8.0, 15.0 x 10^3. The PEG/water system gives a closed-loop phase diagram. Solid lines are calculated; they fit well to experimental data. For this system, we used parameters calculated from LLE data to predict VLE. The results show a big deviation between calculated χ and experiment, probably because the temperature range of our LLE data is much higher than that for our VLE data, or because this system has a strong oriented interaction between polymer and solvent molecules; the latter theory used here does not take such oriented interactions into account. As shown in Table VI, d_0 decreases, while d_1 and d_2 increase with molecular weight of polymer.

Figure 7 shows the χ parameter as a function of composition. We used our χ data to calculate the adjustable parameters shown in Table VI. Solid lines in Figure 7 give calculated χ's using those parameters. Figure 7 shows that our model's composition dependence for χ agrees well with experiment.

Figure 8 shows the cloud-point curves of PS in ethyl acetate. For this system, only an LCST was detected, but we expect that an UCST also exists. Solid lines in Figure 8 are calculated cloud-point curves; they fit experimental data well. In this system, adjustable parameter d_2 is equal to zero since we have only LCST data. Constants d_0 and d_1 have the same trends with molecular weight of polymer as those shown in Table VII.

Figure 9 shows phase diagrams of PS in *tert*-butyl acetate. Both LCST and UCST exist. Calculated curves fit well to experiment. However, there is a slight deviation between calculated and experimental results for the LCST curve. This deviation may be due to the density ("equation of state") effect which is not explicitly taken into account in a lattice theory. The deviation increases with rising temperature.

Figure 10 shows cloud-point curves for PS/methyl acetate. This system also exhibits both LCST and UCST. Calculated curves fit fairly well to the experimental data. Again, there is a slight deviation between calculated values and experimental data for the LCST curve. Constant d_0 increases, while constants d_1 and d_2 decrease with molecular weight of polymer.

Figure 11 shows the cloud-point curves of two polymer-blend systems: PS/poly(vinyl methyl ether) (PVME) for two different molecular weights of PS. This system exhibits LCST. The LCST is lowered with increasing molecular weight of PS as shown in Figure 11. The polydispersity index of PVME ($\overline{M}_w/\overline{M}_n \approx 2.1$) shows that PVME is not a monodisperse polymer and therefore, our equations for a binary system are not truly applicable. Nevertheless, we fit our binary model to experimental data. Solid lines are calculated using the adjustable parameters in Table X. Constant d_2 is equal to zero in this case because the cloud-point data show only LCST. Calculated curves agree well with experiment as shown in Figure 11.

Conclusion

Using a simplified version of the extended Flory-Huggins equation proposed by Qian, Mumby and Eichinger, we have studied VLE and LLE of some binary polymer solutions and LLE for one polymer blend with two different molecular weights for PS. For at least some binary systems, our correlating equation appears to be useful for representing both VLE and LLE using the same adjustable parameters. The model is suitable for several types of phase diagrams.

The extended Flory-Huggins equation presented here has little theoretical basis; it is essentially empirical or, at best, semi-empirical. Its advantage follows from its simplicity; a simple algebraic form with a few adjustable parameters appears to be suitable for representing vapor-liquid and liquid-liquid equilibria, including closed-loop phase diagrams.

Acknowledgment. This work was supported by the Director, Office of Energy Research, Office of Basic Energy Sciences, Chemical Sciences Division of the U.S. Department of Energy under Contract No. DE-AC03-76SF0098. Additional funding was provided by E.I. du Pont de Nemours & Co. (Phil: _hia, PA), Enichem Polimeri (Mantua, Italy) , Koninklijke Shell (Amsterdam, The Netherlands), and ATOCHEM (Paris, France). We are grateful to Mr. Charles Lee for preparing polymer blend films.

References and Notes

(1) P. J. Flory, "Principles of Polymer Chemistry," Cornell University Press, Ithaca, NY 1953.

(2) K. F.Freed, *J. Phys. A: Math. Gen.*, **18**, 871 (1985).

(3) M. G. Bawendi, K. F. Freed, U. Mohanty, *J. Chem. Phys.* ,**87**, 5534 (1987).

(4) M. G. Bawendi and K. F. Freed, *J. Chem. Phys.*, **88**, 2741 (1988).

(5) W. G. Madden, A. I. Pesci, K. F. Freed *Macromolecules*, **23**, 1181 (1990).

(6) W. G. Madden, J. Dudowicz, K. F. Freed *Macromolecules*, **23**, 4803 (1990).

(7) R. Dickman and C. Hall *J. Chem. Phys.*, **85**, 4108 (1988).

(8) Y. Hu, S. M. Lambert, D. S. Soane, J. M. Prausnitz, *Macromolecules* ,**24**, 4356 (1991).

(9) I. C. Sanchez and R. H. Lacombe, *J. Phys. Chem.*, **21**, 2352, 2568 (1976).

(10) I. C. Sanchez and R. H. Lacombe *Macromolecules*, **11**, 1145 (1978).

(11) L. A. Kleintjens and R. Koningsveld,*Colloid Polymer Sci.*, 258, 711 (1980); *Sep. Sci. Tech.* **17**, 215 (1982).

(12) I. C. Sanchez and A. C. Balazs, *Macromolecules*, **22**, 2325 (1989).

(13) C. Panayiotou and I. C. Sanchez, submitted to *Macromolecules*..

(14) P. J. Flory, *J. Am. Chem. Soc.*, **87**, 1833 (1965); *Discuss. Faraday Soc.*, **49**, 7 (1970).

(15) D. Patterson and G. Delmas, *Trans. Faraday Soc.*, **65**, 708 (1969).

(16) C. Qian, S. J. Mumby, B. E. Eichinger, *Macromolecules* , **24**, 1655 (1991).

(17) C. Qian, S. J. Mumby, B. E. Eichinger, *J. Polym. Sci.: Part B* , **29**, 635 (1991).

(18) Cahn Electrobalance manual, Cahn Instrument, Inc.

(19) Y. C. Bae, S. M. Lambert, D. S. Soane, J. M. Prausnitz, *Macromolecules* , **24**, 4403 (1991).

(20) R. Koningsveld and A. J. Staverman, *J. Polym. Sci. Part A-2* , **6**, 305, 325, 349 (1968).

(21) R. Koningsveld, L. A. Kleintjens, A. R. Shultz, *J. Polym. Sci. Part A-2* , **8**, 1261 (1970).

(22) R. Koningsveld and L. A. Kleintjens, *Macromolecules* , **4**, 637 (1971).

(23) K. S. Siow, G. Delmas, D. Patterson, *Macromolecules* , **5**, 29 (1972).

(24) R. J. Orwoll, *Rubber Chem. Technol.* , **50**, 452 (1977).

(25) A. F. M. Barton, "Handbook of Solubility Parameters and Other Cohesion Parameters," CRC Press, Boca Raton, FL 1983.

Table I

Experimental Cloud-Point Data for PS/PVME

PVME ($\overline{M}_w$ = 99,000; $\overline{M}_n$ = 46,500)

MW of PS = 50,000 ($\overline{M}_w/\overline{M}_n$<1.05)		MW of PS = 100,000 ($\overline{M}_w/\overline{M}_n$<1.06)	
W_{ps}	T_L (°C)	W_{ps}	T_L (°C)
0.053	134.4	0.186	142.6
0.104	128.8	0.289	139.2
0.217	125.1	0.409	138.1
0.313	125.0	0.489	138.7
0.411	125.9	0.623	147.0
0.519	129.9	0.711	150.9
0.597	131.5		
0.701	137.5		
0.807	144.3		

W_{ps}: Weight fraction polystyrene

T_L: Lower consolute temperature

Table II

Experimental Cloud-Point Data for PS/Cyclohexane (LCST data)

MW of PS = 100,000 ($\overline{M}_w/\overline{M}_n$ < 1.06)

W_2	T_L (°C)
0.005	238.8
0.007	237.1
0.010	235.1
0.020	231.6
0.030	229.8
0.050	230.7
0.072	229.1
0.102	229.0
0.152	228.8
0.191	229.2
0.251	230.4

W_2: Weight fraction polymer

T_L: Lower consolute temperature

Table III
Experimental VLE Data and χ Parameters for PS/Cyclohexane (MW of PS = 100,000)

30 °C			40 °C		
P/P_1°	W_1	χ	P/P_1°	W_1	χ
0.818	0.150	0.980	0.539	0.062	1.149
0.859	0.178	0.937	0.647	0.087	1.086
0.900	0.215	0.890	0.755	0.136	0.935
0.941	0.262	0.854	0.863	0.195	0.754
0.982	0.401	0.729	0.917	0.255	0.817
			0.971	0.433	0.647

50 °C			60 °C		
P/P_1°	W_1	χ	P/P_1°	W_1	χ
0.367	0.036	1.196	0.665	0.129	0.797
0.550	0.074	1.020	0.767	0.181	0.739
0.642	0.109	0.887	0.844	0.232	0.714
0.733	0.150	0.816	0.895	0.301	0.646
0.825	0.209	0.750	0.946	0.455	0.499
0.917	0.312	0.681			
0.953	0.412	0.607			

P: System pressure
P_1°: Vapor pressure of the solvent
W_1: Weight fraction of solvent

Table IV
Experimental VLE Data and χ Parameters
for PEG/Water (MW of PEG = 8,000)

30 °C			40 °C			40 °C		
$P/P_1°$	W_1	χ	$P/P_1°$	W_1	χ	$P/P_1°$	W_1	χ
0.238	0.014	1.782	0.402	0.027	1.702	0.214	0.008	2.195
0.324	0.021	1.731	0.538	0.049	1.473	0.321	0.017	1.908
0.432	0.032	1.635	0.669	0.091	1.216	0.428	0.028	1.747
0.540	0.061	1.296	0.770	0.197	0.850	0.535	0.056	1.360
0.649	0.103	1.077	0.870	0.302	0.667	0.642	0.077	1.291
0.757	0.189	0.791	0.937	0.495	0.460	0.727	0.110	1.163
0.865	0.355	0.514				0.813	0.197	0.867
0.951	0.584	0.349				0.877	0.290	0.713
						0.941	0.45	0.562

P: System pressure
$P_1°$: Vapor pressure of the solvent
W_1: Weight fraction of solvent

Table V

Adjustable Model Parameters for PS/Cyclohexane

MW of PS	20,400	100,000 (UCST only)	100,000 (LCST & UCST)	610,000
b	0.5144	0.5523	0.5523	0.3872
d_0	-1.1390	-0.5132	-23.51	-0.3503
d_1	460.09	302.05	1307.2	258.99
d_2	0	0	3.4452	0

Table VI

Adjustable Model Parameters for PEG/Water

MW of PEG	3,350	8,000 (from LLE)	8,000 (from VLE)	15,000
b	0.5137	0.4523	0.8750	0.5840
d_0	60.37	46.50	2.3×10^{-7}	25.19
d_1	-3933.5	-3005.2	-137.25	-1619.6
d_2	-8.3581	-6.4178	0.1161	-3.4401

Table VII

Adjustable Model Parameters for PS/Ethyl Acetate

MW of PS	100,000	233,000	600,000
b	0.5922	0.5624	0.5704
d_0	0.8177	0.8053	0.6401
d_1	-133.86	-126.37	-56.67

Table VIII
Adjustable Model Parameters for PS/*tert*-Butyl Acetate

MW of PS	100,000	233,000	600,000
b	0.5507	0.5482	0.5553
d_0	-5.5893	-4.5992	-3.3069
d_1	290.85	245.95	183.76
d_2	0.8961	0.7501	0.5602

Table IX
Adjustable Model Parameters for PS/Methyl Acetate

MW of PS	770,000
b	0.5155
d_0	-3.2850
d_1	192.15
d_2	0.5525

Table X
Adjustable Model Parameters for PS/PVME

MW of PS	50,000	100,000
b	-0.8999	-1.5393
d_0	0.0264	0.0443
d_1	-9.2490	-16.3640

Figure Captions

1. Schematic of the sorption equipment for VLE of polymer solutions (Cahn D-200 electrobalance).
2. Phase diagrams for three polystyrene/cyclohexane systems showing cloud-point temperatures as functions of the weight fraction of polystyrene. Squares, circles, and triangles are for molecular weights 610, 100, and 20.4 x 10^3, respectively. Solid are calculated.
3. Phase diagram for polystyrene/cyclohexane system (MW = 100 x 10^3) showing both UCST and LCST. Solid lines are calculated.
4. χ's for polystyrene/cyclohexane system (MW = 100 x 10^3) as functions of the volume fraction of polymer at four temperatures. Circles, dark triangles, squares, and dark circles are 30, 40, 50, 60 °C, respectively. Solid lines are calculated using adjustable model parameters from UCST LLE data only.
5. χ's for polystyrene/cyclohexane system (MW = 100 x 10^3) as functions of the volume fraction of polymer at four temperatures. Circles, dark triangles, squares, and dark circles are 30, 40, 50, 60 °C, respectively. Solid lines are calculated using adjustable parameters from both UCST and LCST LLE data.
6. Phase diagrams for three poly(ethylene glycol)/water systems showing cloud-point temperatures as functions of the weight fraction of poly(ethylene glycol). Circles, squares, and triangles are for molecular weights 3.35, 8.0 and 15.0 x 10^3, respectively. Solid lines are calculated.

7. χ's for poly(ethylene glycol)/water system (MW = 8.0 x 10^3) as functions of the volume fraction of polymer at three temperatures. Circles, dark triangles, and squares are 50, 60, 70°C, respectively. Solid lines are calculated.
8. Phase diagrams for three polystyrene/ethyl acetate systems showing cloud-point temperatures as functions of the weight fraction of polystyrene. Squares, circles, and triangles are for molecular weights 600, 233, and 100 x 10^3, respectively. Solid lines are calculated.
9. Phase diagrams for three polystyrene/*tert*-butyl acetate systems showing cloud-point temperatures as functions of the weight fraction of polystyrene. Squares, circles, and triangles are for molecular weights 600, 233, and 100 x 10^3, respectively. Solid lines are calculated.
10. Phase diagram for polystyrene/methyl acetate system showing cloud-point temperatures as functions of the weight fraction of polystyrene. Molecular weight of polystyrene is 770 x 10^3. Solid lines are calculated.
11. Phase diagrams for two polystyrene/poly(vinyl methyl ether) systems showing cloud-point temperatures as functions of the weight fraction of polystyrene. Squares and circles are for molecular weights of polystyrene 50 and 100 x 10^3, respectively. Solid lines are calculated.

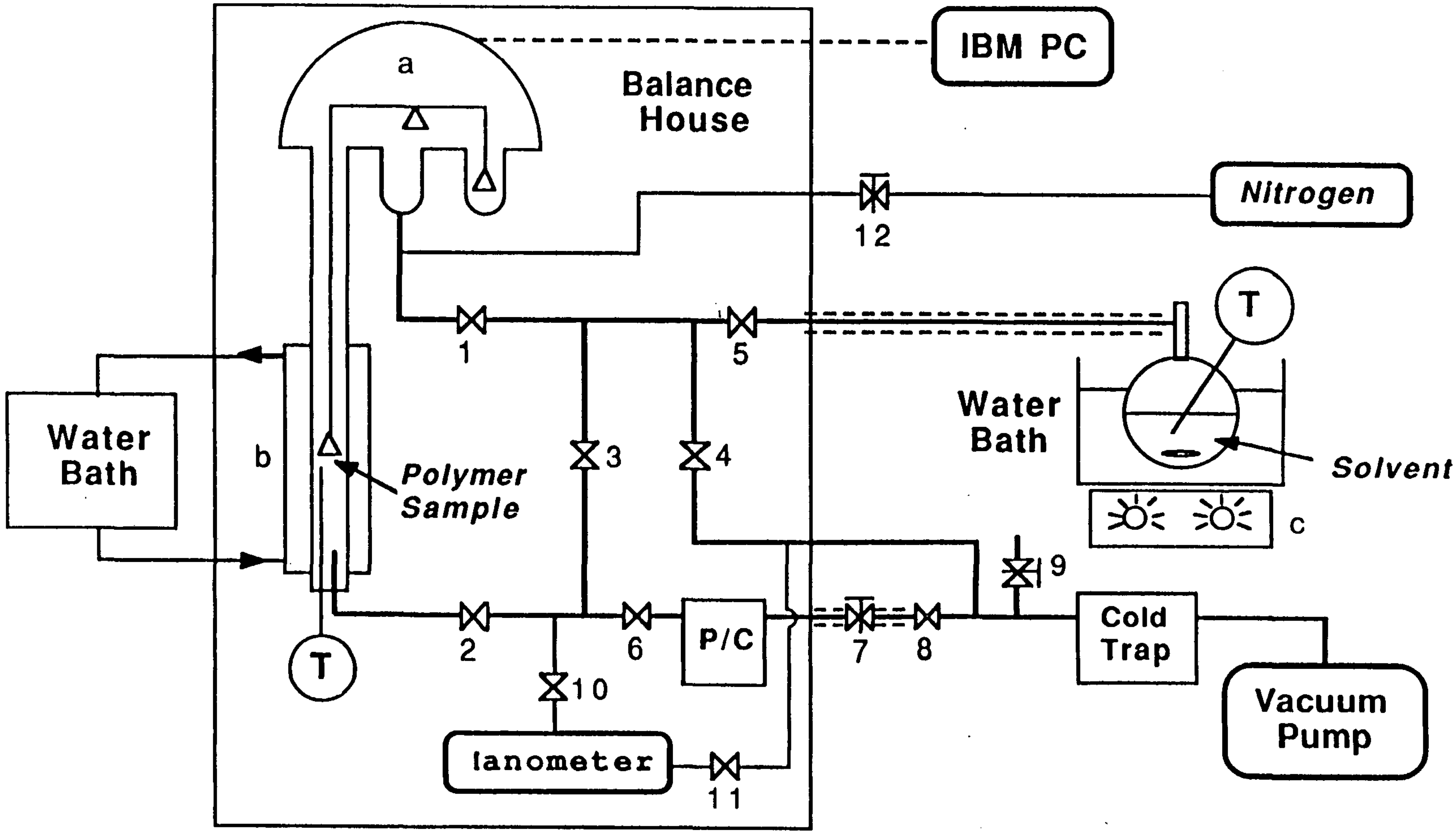

a: Cahn D-200 Electrobalance chamber
b: Hangdown tube-water jacket
c: Magnetic stirrer
-- Heating Tape

1-6,8,10,11: 2-Way ball valve
7,9,12 : Needle valve
T : Thermocouple
P/C: Pressure controller

Figure 1. Schematic of the sorption equipment for VLE of polymer solutions (Cahn D-200 electrobalance).

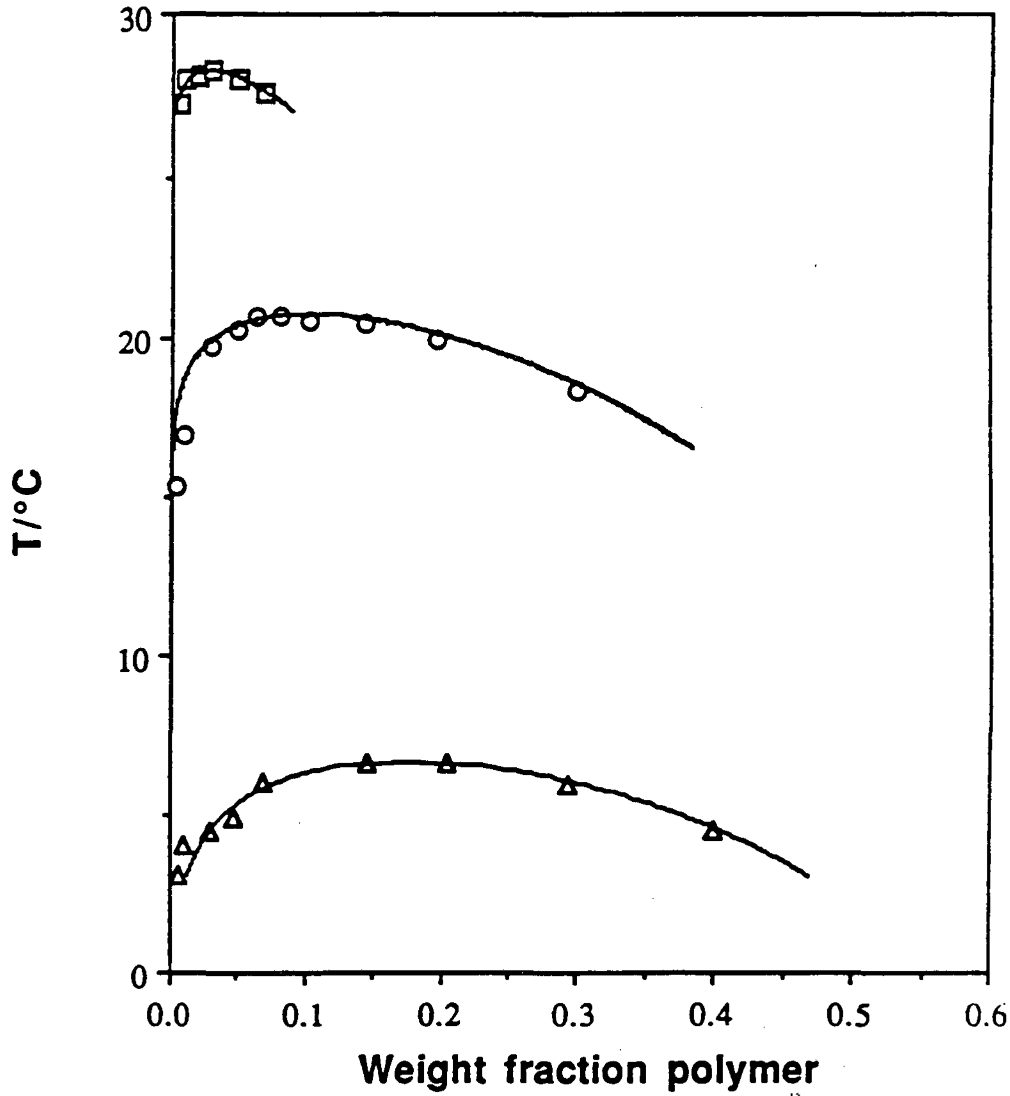

Figure 2. Phase diagrams for three polystyrene/cyclohexane systems showing cloud-point temperatures as functions of the weight fraction of polystyrene. Squares, circles, and triangles are for molecular weights 610, 100, and 20.4 x 10^3, respectively. Solid lines are calculated.

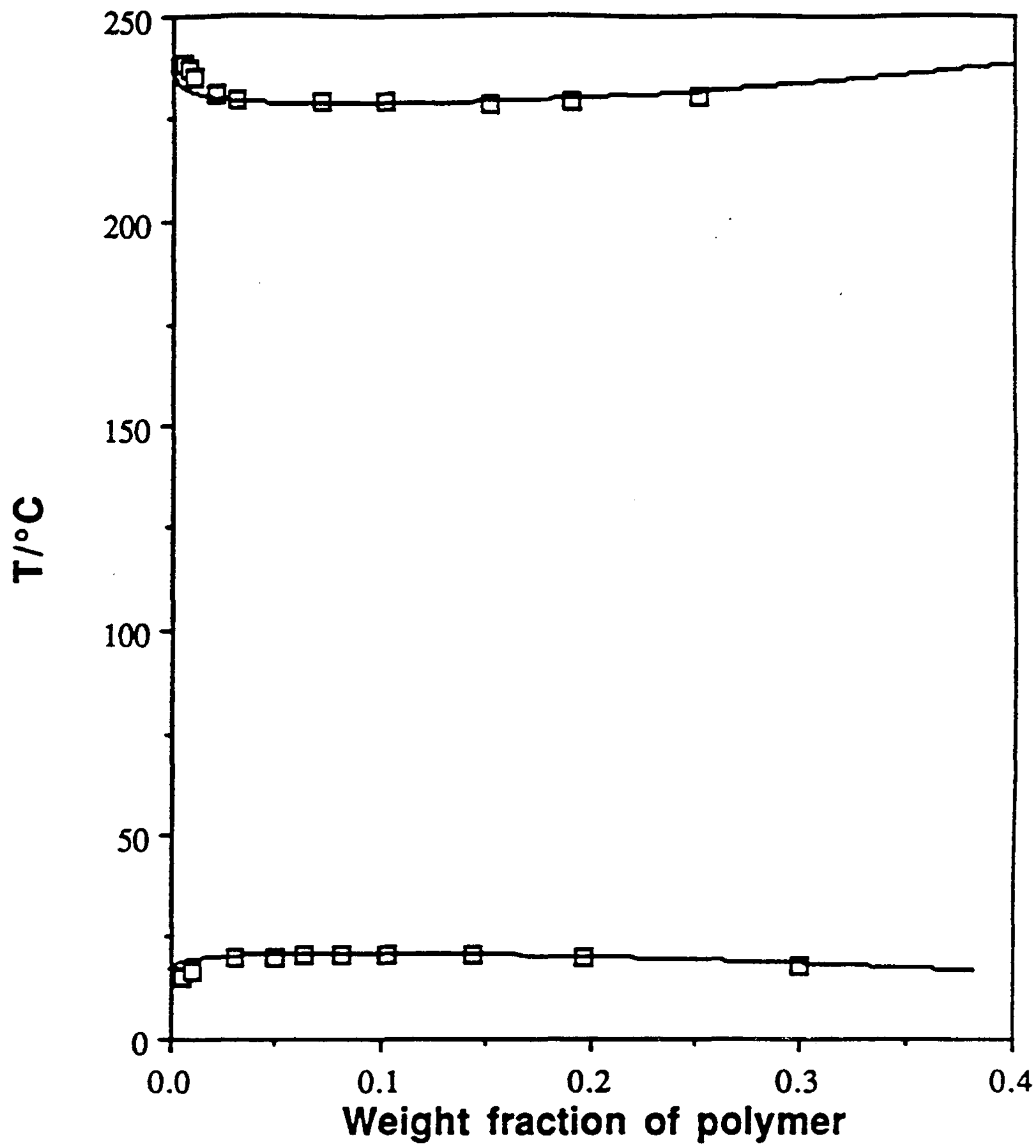

Figure 3. Phase diagram for polystyrene/cyclohexane system (MW = 100 x 10^3) showing both UCST and LCST. Solid lines are calculated.

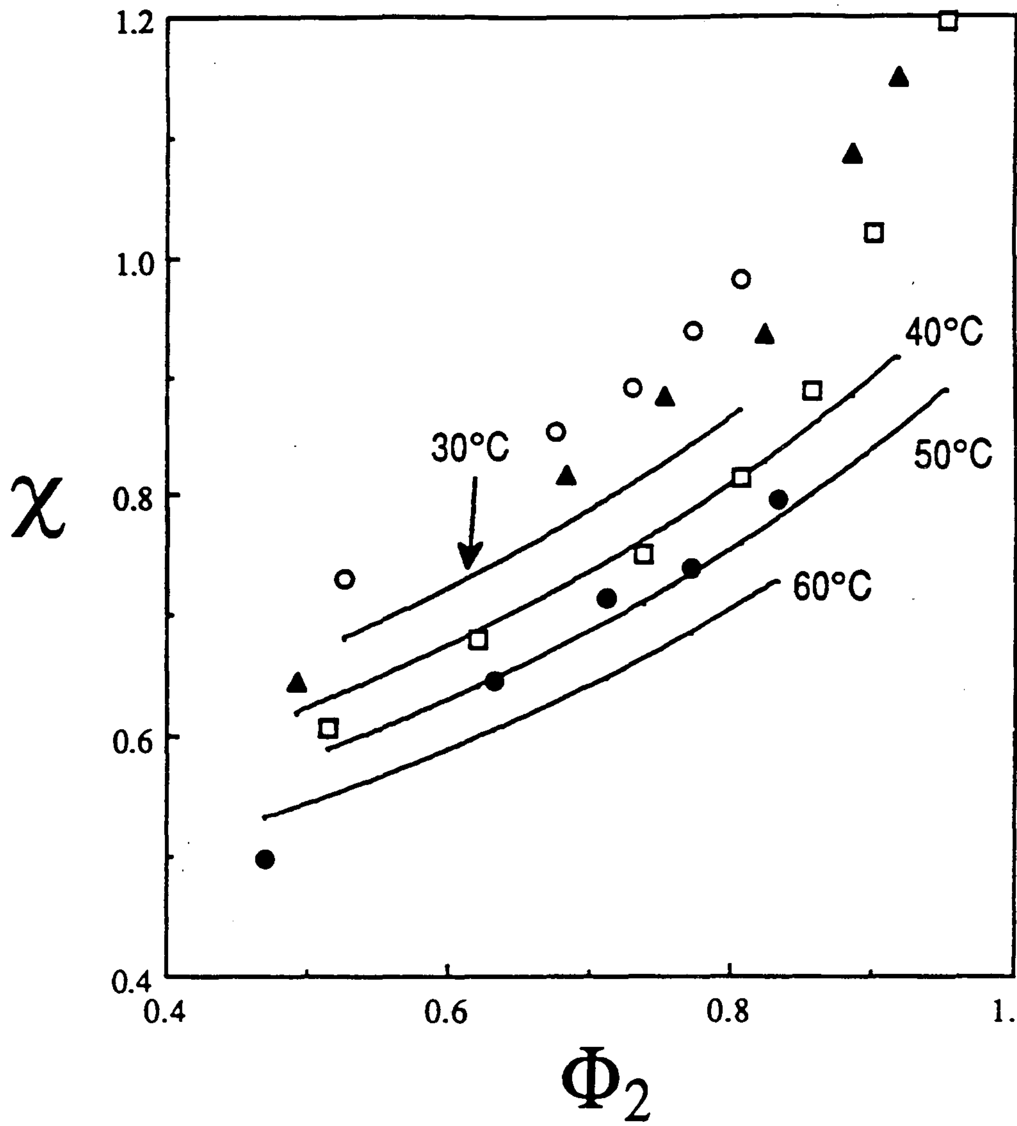

Figure 4. χ's for polystyrene/cyclohexane system (MW = 100 x 10^3) as functions of the volume fraction of polymer at four temperatures. Circles, dark triangles, squares, and dark circles are 30, 40, 50, 60 °C, respectively. Solid lines are calculated using adjustable model parameters from UCST LLE data only.

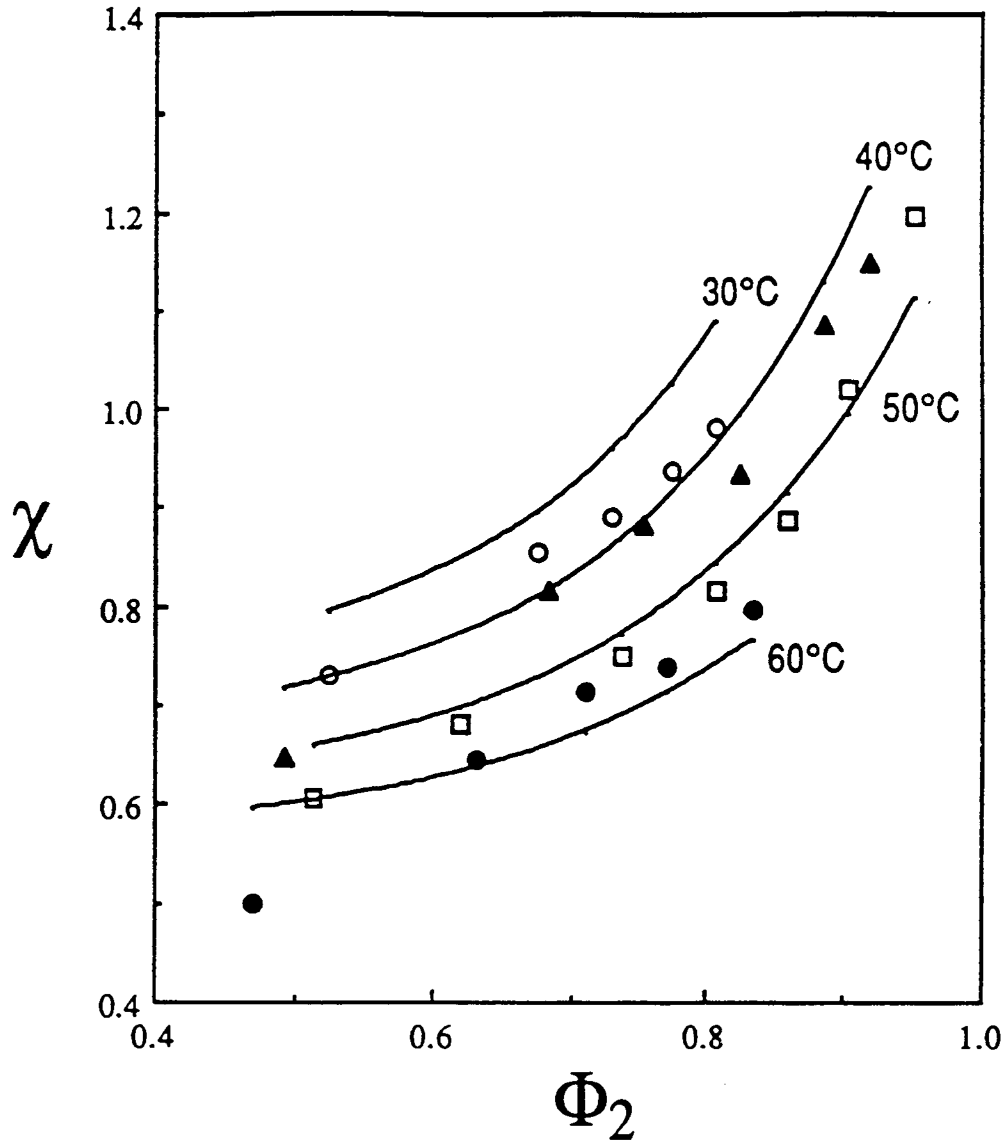

Figure 5. χ's for polystyrene/cyclohexane system (MW = 100 x 10^3) as functions of the volume fraction of polymer at four temperatures. Circles, dark triangles, squares, and dark circles are 30, 40, 50, 60 °C, respectively. Solid lines are calculated using adjustable parameters from both UCST and LCST LLE data.

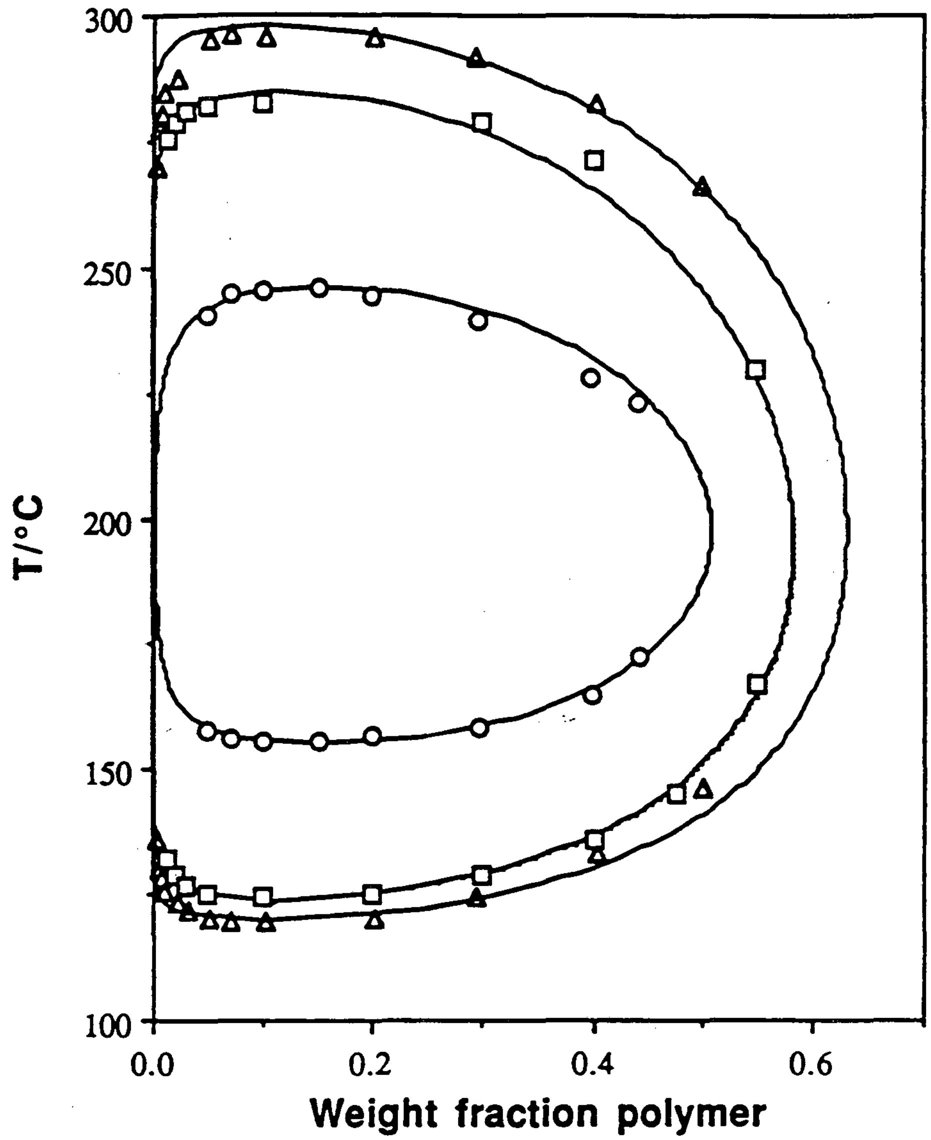

Figure 6. Phase diagrams for three poly(ethylene glycol)/water systems showing cloud-point temperatures as functions of the weight fraction of poly(ethylene glycol). Circles, squares, and triangles are for molecular weights 3.35, 8.0 and 15.0 x 10^3, respectively. Solid lines are calculated.

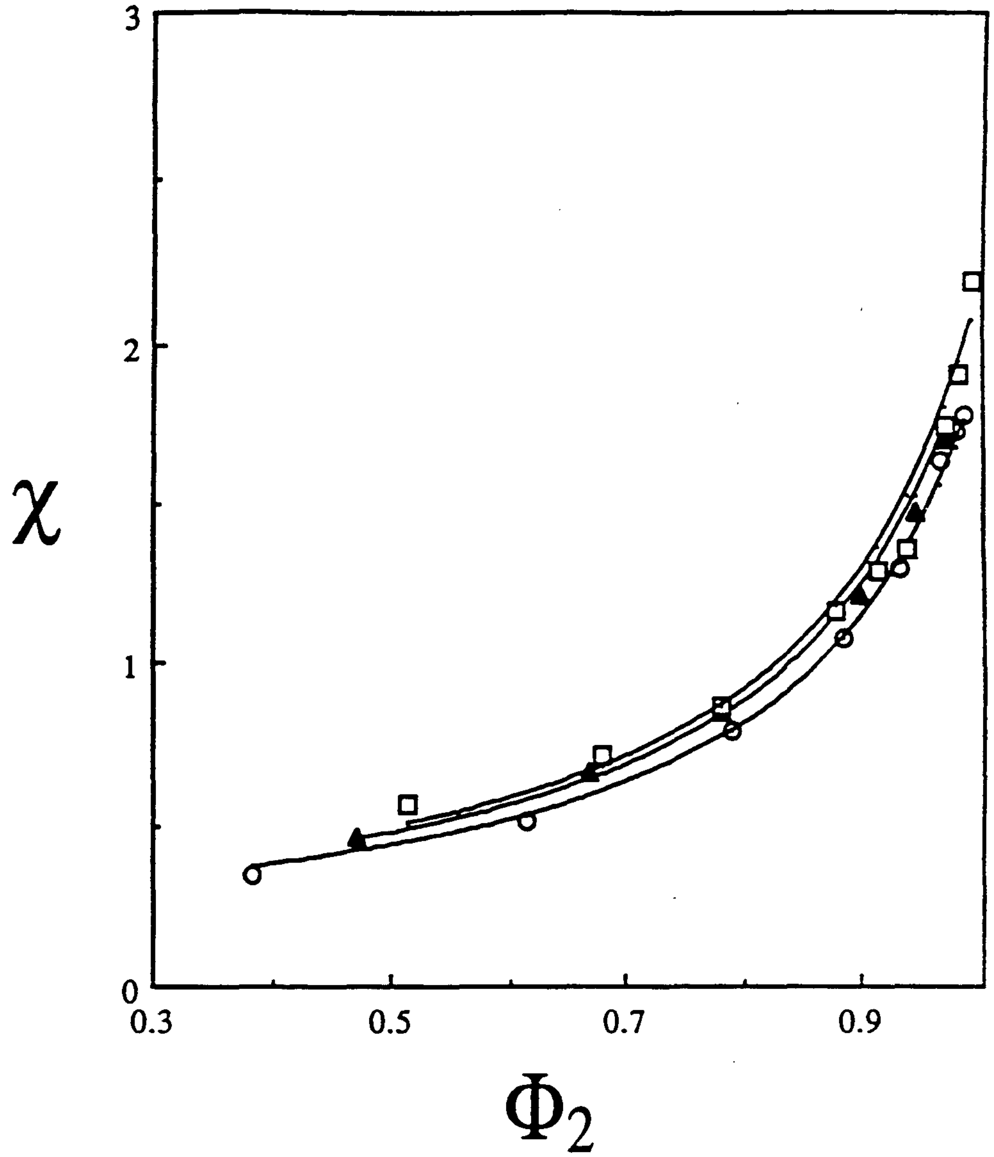

Figure 7. χ's for poly(ethylene glycol)/water system (MW = 8.0 x 10^3) as functions of the volume fraction of polymer at three temperatures. Circles, dark triangles, and squares are 50, 60, 70 °C, respectively. Solid lines are calculated.

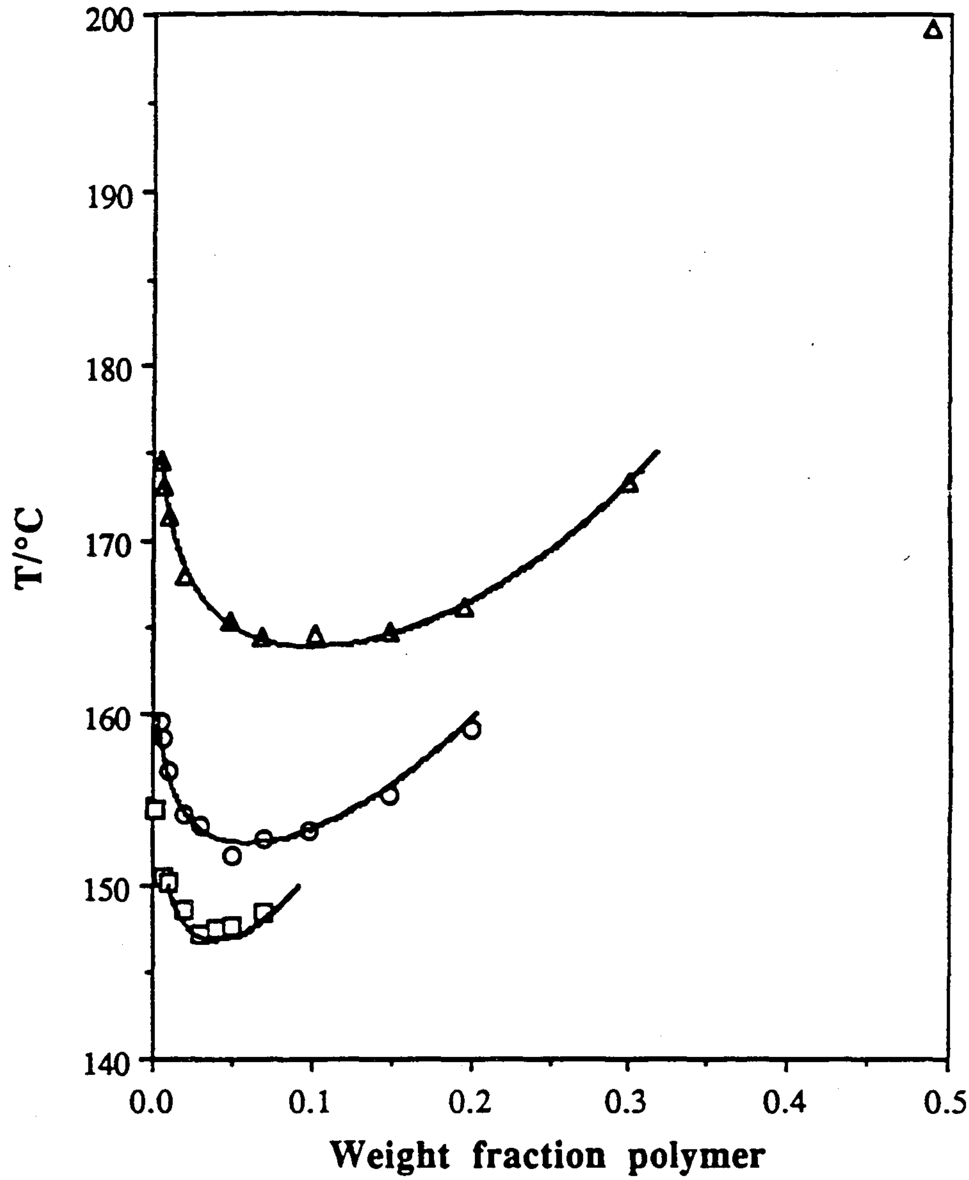

Figure 8. Phase diagrams for three polystyrene/ethyl acetate systems showing cloud-point temperatures as functions of the weight fraction of polystyrene. Squares, circles, and triangles are for molecular weights 600, 233, and 100 x 10^3, respectively. Solid lines are calculated.

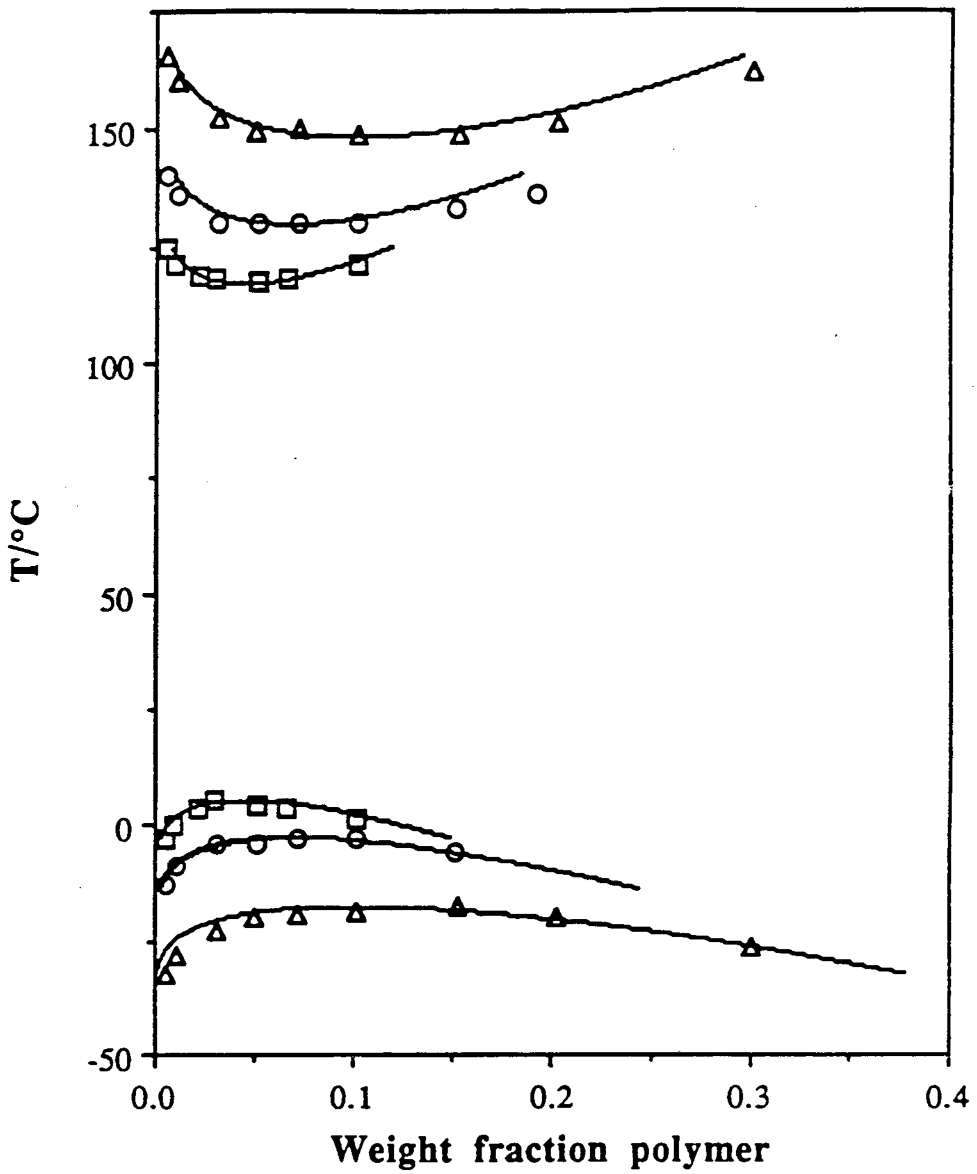

Figure 9. Phase diagrams for three polystyrene/*tert*-butyl acetate systems showing cloud-point temperatures as functions of the weight fraction of polystyrene. Squares, circles, and triangles are for molecular weights 600, 233, and 100 x 10^3, respectively. Solid lines are calculated.

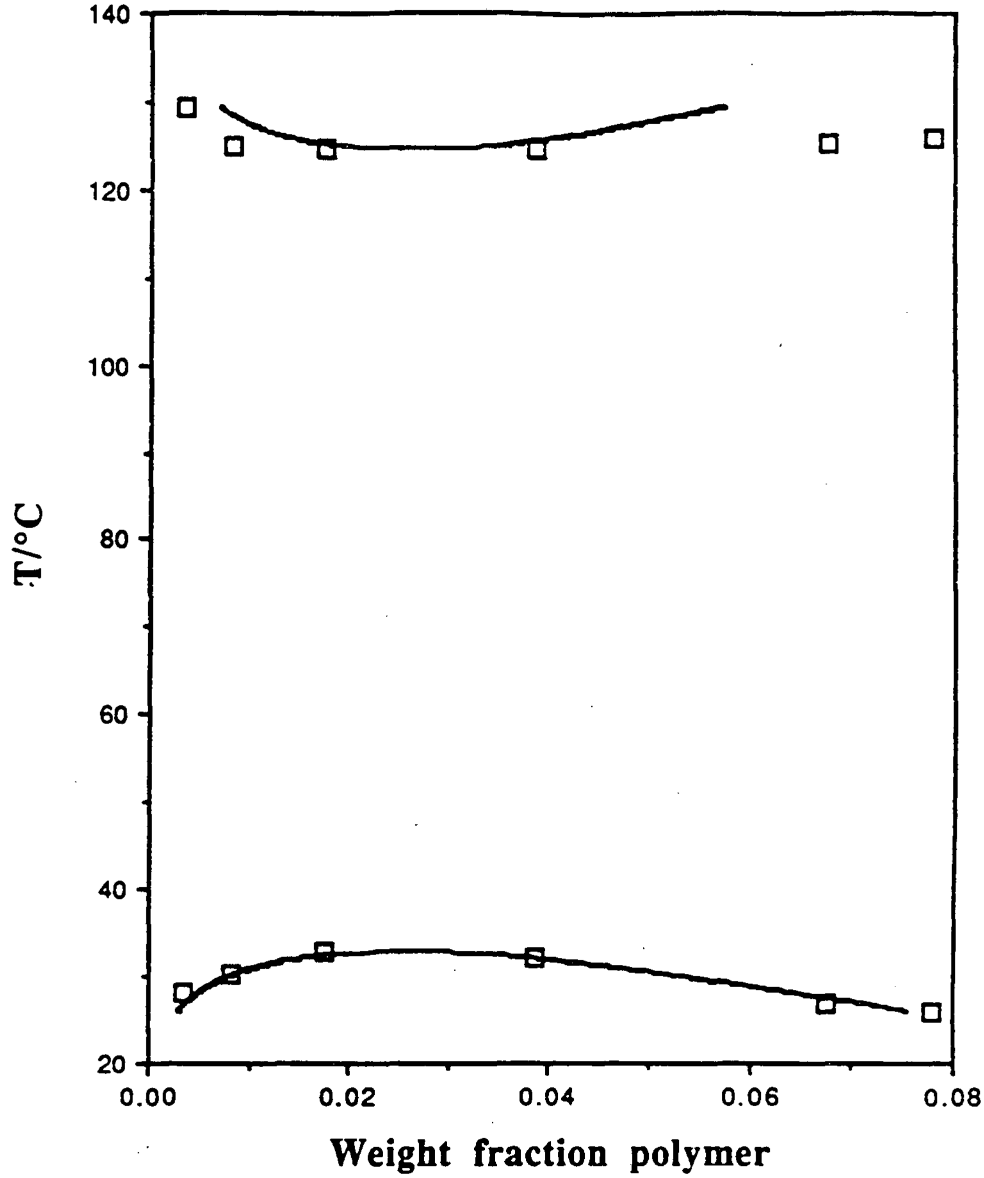

Figure 10. Phase diagram for polystyrene/methyl acetate system showing cloud-point temperatures as functions of the weight fraction of polystyrene. Molecular weight of polystyrene is 770 x 10^3. Solid lines are calculated.

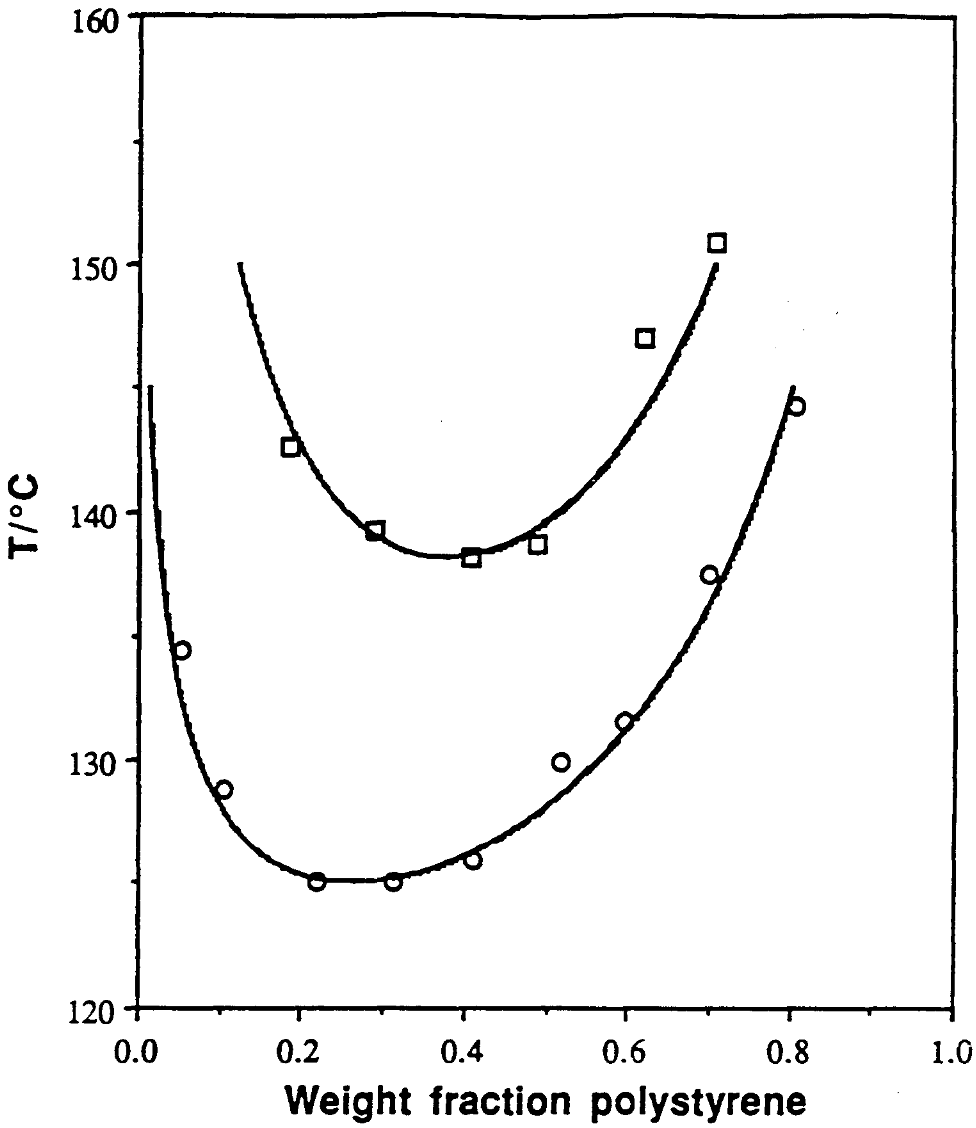

Figure 11. Phase diagrams for two polystyrene/poly(vinyl methyl ether) systems showing cloud-point temperatures as functions of the weight fraction of polystyrene. Squares and circles are for molecular weights of polystyrene 50 and 100 x 10^3, respectively. Solid lines are calculated.

LAWRENCE BERKELEY LABORATORY
UNIVERSITY OF CALIFORNIA
TECHNICAL INFORMATION DEPARTMENT
BERKELEY, CALIFORNIA 94720